WATER RESOURCES RESEARCH, VOL. 37, NO. 1, PAGES 165–170, JANUARY 2001

# Pore-scale modeling extension of constitutive relationships in the range of residual saturations

Rudolf J. Held and Michael A. Celia

Environmental Engineering and Water Resources Program, Department of Civil and Environmental Engineering
Princeton University, Princeton, New Jersey

**Abstract.** A pore network model is used to describe constitutive relationships between saturation, capillary pressure, relative permeabilities, and interfacial areas over the full range of saturations. We focus on residual nonwetting-phase saturations, that is, the saturation range between main drainage and primary drainage. Interphase mass transfer and dynamic miscible transport are modeled to generate the range of saturations over which the extended constitutive relationships are calculated. To accommodate all saturations in a consistent way, we define capillary pressure as the areal average of local capillary pressures associated with each fluid-fluid interface. The extended constitutive relationships provide input for continuum-scale models covering the entire saturation range and indicate that special care is needed in the general formulation of continuum-scale equations.

## 1. Introduction

Mathematical descriptions of multiphase fluid flow in porous media are based on conservation laws, including conservation of mass and momentum. These are augmented by constitutive relationships between capillary pressure ($p^c$) and saturation ($s^w$) and between relative permeability ($k_r$) and saturation. For problems involving mass exchange between the phases, additional balance equations, including those for specific components of interest, need to be written. Additional constitutive relationships are also required. These constitutive relationships typically involve a measure of fluid-fluid interfacial area ($a^{wn}$). An example of this is the dissolution of a nonaqueous phase liquid (NAPL) into flowing groundwater [see, e.g., *Miller et al*., 1998, and references therein]. Interfacial area has also been highlighted recently [*Hassanizadeh and Gray*, 1990; *Gray and Hassanizadeh*, 1991, 1998] as a fundamental quantity in the mathematical system description. That work suggests that interfacial area should be related thermodynamically to both saturation and capillary pressure. *Reeves and Celia* [1996] presented a relationship between $p^c$, $s^w$, and $a^{wn}$ obtained by pore-scale network models, showing the relationship to be a smooth, well-behaved surface. In this study, we present further computations of the relationship between capillary pressure, saturation, relative permeability, and interfacial area, with a focus on the range of residual nonwetting-phase saturation. In this range, saturation changes are caused by mass transfer processes from the nonwetting phase into the wetting phase.

One of the interesting observations regarding capillary pressure is that its definition at the continuum scale is not unique. At the pore scale, capillary pressure is well defined, being equal to the difference between the pressure of the nonwetting fluid and the pressure of the wetting fluid, measured across a fluid-fluid interface. This concept is translated to the macroscopic porous-medium scale by use of the rather loose definition that average capillary pressure is the difference between the nonwetting- and wetting-phase pressures. When performing laboratory pressure cell experiments to determine the $p^c - s^w$ relationship, values of $p^c$ are usually taken as the difference between imposed wetting- and nonwetting-phase pressures at the boundary of the cell. Sufficient time is assumed so that the pressures of the respective fluids within the sample are equilibrated to the imposed external pressures. However, for regions where fluids in the sample become disconnected from the pressure-controlling external reservoir, the isolated fluid may no longer exhibit the pressure of its external reservoir. Arguments about wetting films can be employed to mitigate this effect during drainage, although one is left with questions about timescales, dynamic effects, and the existence of a residual wetting-phase saturation (see, e.g., *Dullien et al*. [1986] for experiments and discussion in this regard). In imbibition all of the trapped nonwetting phase remains in the sample as isolated fluid, and therefore the external reservoir pressure becomes meaningless for the description of this trapped fluid. Under these conditions, actual internal pressures should be used to define capillary pressure, instead of external reservoir pressures.

This technical note presents computational results, based on an extension of the pore-scale network model of *Reeves and Celia* [1996] and *Reeves* [1997]. Through use of the expanded model we compute capillary pressures, interfacial areas, and relative permeabilities for saturations where the nonwetting phase exists as disconnected ganglia. This is accomplished through implementation of a computational algorithm for dissolution of the nonwetting phase into the wetting phase. A consistent definition of capillary pressure allows the traditional $p^c - s^w$ and $k_r - s^w$ curves to be extended to the range of disconnected nonwetting fluid. The network model gives the added benefit of direct computation of interfacial areas and the relationship between $a^{wn}$ and $s^w$.



Paper number 2000WR900234.
0043-1397/01/2000WR900234$09.00

## 2. Definition of Capillary Pressure

Traditional definitions of capillary pressure are given in terms of macroscale quantities that are readily measurable,

like the difference in pressures at the external fluid-phase boundaries. Such definitions of external capillary pressure lack a thermodynamic relation to the properties of the system [*Hassanizadeh and Gray*, 1993b]. While various thermodynamic definitions of capillary pressure exist [see, e.g., *Morrow*, 1970; *Hassanizadeh and Gray*, 1993b], they often include variables like Helmholtz free energies that are difficult to quantify or measure. Here we adopt a more intuitive definition of capillary pressure where we define macroscale capillary pressure in terms of microscale variables (following *Hassanizadeh and Gray* [1993b] and *Reeves* [1997]) as the areal average of local capillary pressures, where the local pressures can be quantified at the pore scale for each fluid-fluid interface and the averaging is performed over all interfaces. This may be written mathematically as

$$\langle p^c(t)\rangle^{wn} = \frac{1}{\delta A^{wn}(t)} \int_{\delta V^{wn}} (p^n(\mathbf{x}, t) - p^w(\mathbf{x}, t))|\nabla I(\mathbf{x}, t)|\, d\mathbf{x}, \tag{1}$$

where

$$I(\mathbf{x}, t) = \begin{cases} 1, & \mathbf{x} \in w(t) \\ 0, & \mathbf{x} \in n(t), \end{cases} \tag{2}$$

with $w(t)$ and $n(t)$ denoting the portion of space occupied by wetting and nonwetting fluid, respectively. $I(\mathbf{x}, t)$ is an indicator function for the fluid phases in space and time, with $\mathbf{x}$ being a position vector and $t$ indicating time. Local phase pressures are identified by $p^n$ (nonwetting phase) and $p^w$ (wetting phase), $\delta A^{wn}(t)$ is the total contact area between the fluid phases in time, and $\delta V^{wn}$ is the total volume of fluid phases within the averaging volume $\delta V$. In this notation, $a^{wn}$, the specific interfacial area per unit total volume $\delta V$, may be expressed as

$$\langle|\nabla I(\mathbf{x}, t)|\rangle = \frac{1}{\delta V} \int_{\delta V^{wn}} |\nabla I(\mathbf{x}, t)|\, d\mathbf{x} = a^{wn}(t). \tag{3}$$

In our computations we first simulate a typical pressure cell experiment used to determine the relationship between $p^c$ and $s^w$. For such experiments, fluid pressures are imposed at the boundaries of the cell via connection to respective fluid reservoirs. Fluids move in response to imposed differences in phase pressures, and after fluid-fluid interfaces reach stable positions, the corresponding saturation value is associated with the appropriate external capillary pressure. All capillary pressures reported in this work are based on the local pressures appearing in the integrand of (1). Specific algorithms are implemented to calculate fluid pressure differences at interfaces during a dissolution process, as discussed in section 3. Equation (1) is then computed in a discrete form with

$$\langle p^c(t)\rangle^{wn} = \frac{1}{\sum A^{wn}(t)} \sum_{i=1}^{N(t)} (p^n - p^w)_i A_i^{wn}, \tag{4}$$

where $N$ denotes the total number of fluid-fluid interfaces within $\delta V$ at a given time and the summation is performed over all interfaces within $\delta V$. The same holds for (3), i.e., $a^{wn}(t) = \Sigma A^{wn}(t)/\delta V$.

## 3. Methods

The pore-scale network model is based on the basic fluid displacement model developed by *Reeves and Celia* [1996] and *Reeves* [1997]. It represents the pore space by a cubic lattice of spherical pore bodies, connected by biconical pore throats (Figure 1). The radii of the pore bodies are assigned randomly according to a beta distribution with upper and lower size limits. Pore throat radii are correlated in size to the connecting pore bodies, following *Reeves* [1997].

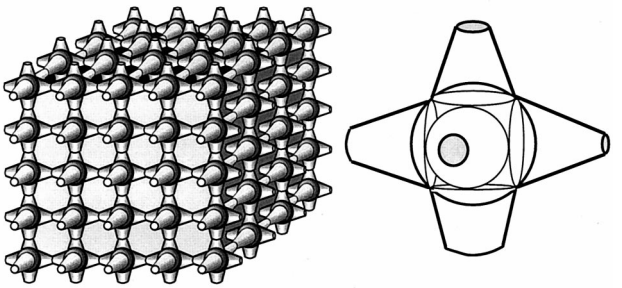

**Figure 1.** (left) Schematic of cubic lattice network and (right) single pore space unit (similar to *Ewing and Gupta* [1994]). The pore space is composed of spheres (bodies) and converging conical sections (throats).

For externally imposed phase pressures the model tracks individual fluid-fluid interfaces in the network, determining their stable position by the Young-Laplace equation. When stable positions are found for all interfaces under a given pressure difference, corresponding volumes occupied by each phase can be calculated for a given pore geometry. This provides a data point for the $p^c - s^w$ relationship, as in a pressure cell experiment. In addition to explicit tracking of all the interfaces, the algorithm identifies regions of resident fluid that become trapped by the displacing phase. Once a region or ganglion of isolated fluid forms in drainage or imbibition, it is considered to remain disconnected.

All interfaces associated with a region of trapped fluid are assigned a fixed capillary pressure, which is the capillary pressure at entrapment. This is in agreement with observations of *Harris and Morrow* [1964] and *Morrow and Harris* [1965]. For imbibition, isolated nonwetting fluid is held at a fixed capillary pressure until either a drainage sequence is initiated, where invading nonwetting fluid reconnects to the ganglion, or mass transfer (dissolution) between fluid phases occurs. During dissolution, capillary pressures are modified for each ganglion, based on the new positions of interfaces, which are obtained from the nonwetting-phase volume dissolved and the local pore geometry. The dissolved volume is calculated in connection with aqueous-phase mass transport across the network, with each fluid-fluid interface treated as a source for mass transfer, driven by local concentration gradients. The dissolved mass converts to a NAPL volume reduction, assuming incompressible nonaqueous phase. With this adjustment, interface locations and interface curvatures need to change in the pore space geometry. Therefore local capillary pressure also changes. Finally, (4) is used to calculate a new value of average $p^c$. Physical processes such as snap off [see, e.g., *Li and Wardlaw*, 1986a, 1986b; *Mohanty et al*., 1987] are simulated in ganglion retraction, and minimum energy principles are applied to specific interface configurations. These mechanisms give rise to dynamic ganglia dissolution, and discrete capillary pressure and interfacial area dependence, in the pore network structure.

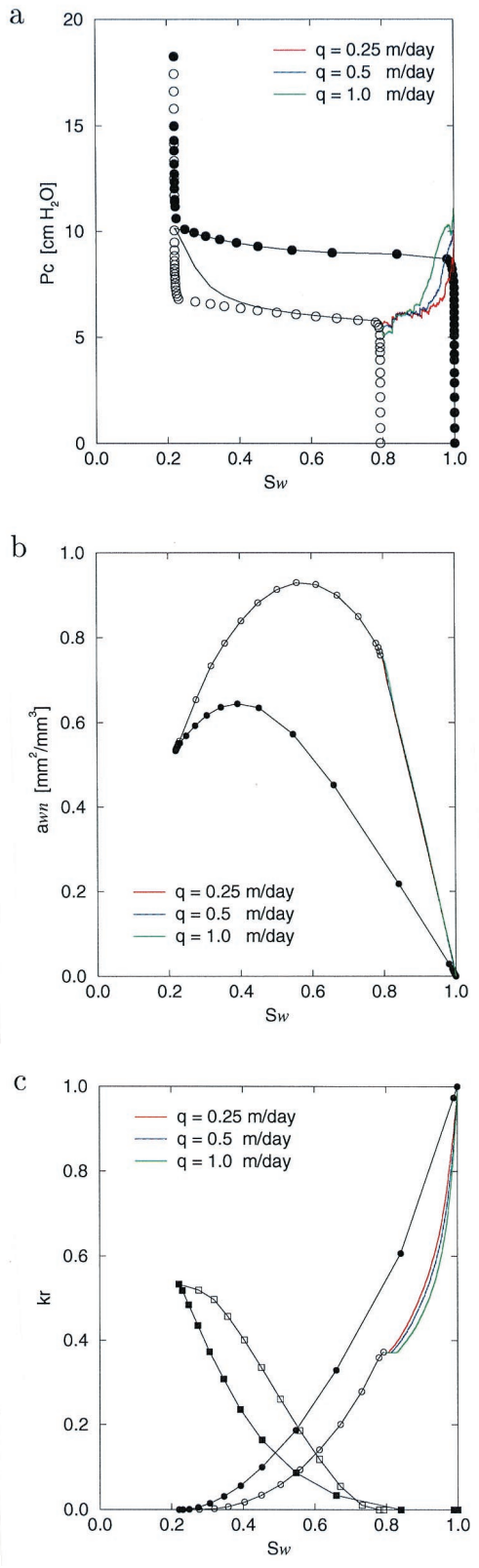


Details of the dissolution algorithm are given by *Held and Celia* [2000].

When nonwetting phase (as part of a ganglion or as single droplet) occupies only a fraction of a pore body, interfacial area and curvature are related to a sphere of the same volume (minimizing interfacial area) in the computation. This provides a lower bound on interfacial area and a respective upper bound on the associated capillary pressure via interfacial curvature. The resulting equation for the pore bodies, which follows from the Young-Laplace equation, reads

$$(p^n - p^w)_i \leq 2\gamma^{wn}/(R_{\text{eq}})_i, \tag{5}$$

where $R_{\text{eq}} = \sqrt{A_{\text{eq}}/4\pi}$ for an equivalent sphere, with $A_{\text{eq}}$ denoting surface area of the sphere. If that nonwetting phase volume in a pore body is still connected to pore throats occupied by nonwetting fluid, then $A_{\text{eq}}$ in this formulation is required to equal at least the combined entrance area of these pore throats. Interfaces that reside in pore throat geometries can be related to a capillary pressure through the Young-Laplace equation directly.

With the updated positions for every interface of the ganglia a new saturation value may be computed for the pore network, as well as an average capillary pressure and a new specific interfacial area. Saturation changes also affect the relative permeability ($k_r$) of the porous medium to the wetting phase (the isolated nonwetting phase has zero relative permeability). This relative permeability can be calculated within the model. A sequence of such calculations, as the dissolution process continues, provides the data points for the extended relationships between $p^c$ and $s^w$, $k_r$ and $s^w$, and $a^{wn}$ and $s^w$.

## 4. Numerical Experiments

In the model setup a wetting-phase reservoir is in contact with the inflow boundary of the network, while a nonwetting-phase reservoir is in contact with the outflow boundary, for simulation of drainage and imbibition displacement followed by nonwetting-phase dissolution. The four lateral boundaries are no-flow. The effects of gravity are not taken into account; that is, the setup may be viewed as horizontal. External reservoir pressures control the drainage and imbibition processes. The network model simulates quasi-static responses to each incremental change in reservoir pressures. This procedure gives the characteristic $p^c - s^w$, $a^{wn} - s^w$, and $k_r - s^w$ relationships, as shown in Plate 1. Commonly capillary pressure $p^c$ is taken to be $p^n_{\text{res}} - p^w_{\text{res}}$, where subscript "res" denotes fluid reservoir pressure. This is also plotted in Plate 1a. The definition of $p^c$ used herein (see (1) and (4)) is not based on the imposed external reservoir pressures but, instead, on

**Plate 1.** (Opposite) Network model prediction of extended constitutive relationships during dissolution of residual nonwetting phase, with a network size of 50 × 50 × 50. Solid symbols represent drainage, and open symbols represent imbibition. The extensions are given for three values of wetting phase Darcy fluxes during the dissolution process: (a) Saturation–capillary pressure relationship. Symbols indicate the difference in phase reservoir pressures; lines indicate the average over local capillary pressures (equation (1)). (b) Saturation–interfacial area relationship. (c) Saturation–relative permeability relationship. Square symbols indicate nonwetting phase permeability; circles indicate wetting phase permeability.

**Table 1.** Model Parameters of Numerical Experiment

| Parameter | Value |
|---|---|
| Pore site radii distribution $\beta$ | |
| Mean | 0.094 mm |
| Standard deviation | 0.014 mm |
| Minimum | 0.05 mm |
| Maximum | 0.12 mm |
| Lattice spacing $d$ | 0.3 mm |
| Sample porosity $\varepsilon$ | 0.312 |
| $H_2O$ density $\rho^w$ | 998 g/L |
| $H_2O$ viscosity $\mu^w$ | 1.0 cP |
| TCE density $\rho^n$ | 1465 g/L |
| TCE viscosity $\mu^n$ | 0.58 cP |
| Surface tension $\gamma^{wn}$ | 35.0 dyn/cm |
| TCE solubility in $H_2O$ $C_S^w$ | 1280 mg/L |
| Molecular diffusivity in $H_2O$ $D_m$ | $1.0 \times 10^{-9}$ m$^2$/s |
| Darcy flux $q$ | 0.25, 0.5, 1.0 m/d |

the average over all fluid-fluid interfaces. As saturation approaches residual phase saturation, this value deviates from the external reservoir pressures. This can be noted as wetting-phase saturation approaches residual at the end of the drainage sequence and as nonwetting phase approaches residual at the end of the imbibition sequence. At irreducible wetting-phase saturation all fluid-fluid interfaces are fixed, and the averaged $p^c$ does not extend beyond $p^c = 10$ cm $H_2O$, independent of external wetting-phase reservoir pressures. Contrary to results based on phase reservoir pressures, the value of $p^c$ thus remains bound at irreducible water saturation. As the wetting fluid reconnects with its reservoir during imbibition, the average $p^c$ gradually approaches the value of the external pressure reservoirs in the midsaturation ranges. The averaged local $p^c$ values then deviate again as the nonwetting phase in the system becomes disconnected.

Once the nonwetting phase reaches residual saturation, further reductions in its saturation can occur by mass transfer and dissolution. While the definition of $p^c$ based on phase reservoir pressures is meaningless in this range of saturations, the formulation of (1) remains well defined and can be employed to define an extended $p^c - s^w - a^{wn}$ relationship over the entire range of saturations. To this end, after residual nonwetting-phase saturation is established, continuous wetting-phase flow is simulated by controlling wetting-phase pressure at the open boundaries. Clean water is introduced at the inflow boundary, serving to flush out dissolving nonwetting phase. The dissolution algorithm is described by *Held and Celia* [2000]. Initially, the aqueous-phase concentration throughout the network is set equal to the solubility limit. The flushing produces a dissolution front that propagates through the network. For this work, we varied the hydraulic gradient in the aqueous phase to simulate Darcy fluxes across the sample between 0.25 m/d and 1 m/d, representing different flow rates during dissolution scenarios or water flooding. The selected flow rates are typical of flow rates in aquifer material. Hydraulic gradients in the model are updated in the simulations to maintain the specified flux condition. Model parameters used in our simulations are compiled in Table 1.

### 4.1. Extended Capillary Pressure Relationship

Areally averaged capillary pressures (equation (1)) give well-defined capillary pressures over the entire range of saturations. Therefore the $p^c - s^w$ relationship can be extended into the region of isolated fluid ganglia. We present such an extended functional relationship in Plate 1a. The extension of the curve corresponding to dissolution is less smooth than for displacement, because of the variability of pressures associated with trapped ganglia at residual saturations. This is a combined effect of the variability in capillary pressures at which the ganglia are originally trapped and dynamic conditions during the dissolution process. More than 5000 ganglia were initially present at residual saturation, inside a pore network of 1.5 cm cubed or 50 pores across each side. Table 2 provides the statistics for the capillary pressures at the point of entrapment for each nonwetting-phase ganglion. Interfaces close to the wetting fluid reservoir became entrapped, on average, at a higher external pressure and vice versa for interfaces close to the nonwetting reservoir. The sequence in which the isolated nonwetting-phase regions dissolve determines the average pressure over the remaining interfaces.

A notable consequence of the local definition for $p^c$ is that the relationship between $p^c$ and $s^w$ is no longer monotonic over its entire range. While this can be explained physically, with shrinking droplets that will have an increasing $p^c$, mathematically it may create difficulties if the extended relationship is used in standard two-phase flow equations at the macroscopic level. When the wetting-phase equation is solved for pressures and $s^w$ is assumed to be a function of $p^c$, then derivatives of $s^w$ with respect to $p^c$ will appear in the equation. A change of sign in the derivative may lead to instability in the solution. Equations should thus be formulated to avoid use of these derivatives in the range of residual phases.

### 4.2. Interfacial Area Relationship

As opposed to pressure cell experiments, wherein measurement of $a^{wn}$ is extremely difficult, the computational network model allows interfacial areas to be calculated directly. Specific interfacial area (defined in (3)) is plotted as a function of saturation in Plate 1b, presenting an extension into the saturation range corresponding to nonwetting-phase dissolution. The curve shows a very well behaved functional relationship, with the area decreasing monotonically to zero as residual saturation decreases to zero. Interfacial area does not enter into standard macroscale two-phase flow equations, but it does appear in the equations for mass transfer. It also appears in the set of two-phase flow equations proposed by *Hassanizadeh and Gray* [1993a]. The form of the functional dependence shown in

**Table 2.** Residual Nonwetting Phase Distribution[a]

| Parameter | Mean | Standard Deviation | Minimum | Maximum | Unit |
|---|---|---|---|---|---|
| Ganglia capillary pressure $\langle p^c \rangle^j$ | 5.855 | 0.212 | 5.454 | 7.712 | cm $H_2O$ |
| Ganglia fluid-fluid area, $\Sigma_{i\in j}\, a_i^{wn}$ | $3.791 \times 10^{-1}$ | 1.828 | $7.341 \times 10^{-2}$ | $9.895 \times 10^{2}$ | mm$^2$ |
| Ganglia total area, $\Sigma_{i\in j}\, (a_i^{wn} + a_i^{ns})$ | $7.719 \times 10^{-1}$ | 4.482 | $9.714 \times 10^{-2}$ | $2.422 \times 10^{3}$ | mm$^2$ |
| Ganglia volume, $\Sigma_{i\in j}\, V_i^n$ | $3.288 \times 10^{-2}$ | $1.967 \times 10^{-1}$ | $3.521 \times 10^{-3}$ | $1.063 \times 10^{1}$ | mm$^3$ |

[a]Total number of nonwetting phase ganglia is 5032.

Plate 1b is in full agreement with the hypothesized relationship of *Hassanizadeh and Gray* [1993b]. Other results, not presented herein, indicate that less smooth curves for $a^{wn} - s^w$ may be generated, depending on specific pore structures of the systems. However, the general trends remain consistent. Our simulated wetting-nonwetting fluid interfacial areas are less in magnitude than those estimated by *Gvirtzman and Roberts* [1991] and *Lowry and Miller* [1995] or those inferred by *Saripalli et al*. [1998]. That effect may be attributed to the use of different pore structures and to the absence of wetting films or pendular rings, which carry additional area, although that area probably has a minor effect on the mass-transfer process. Note also that the interfacial area curves shown in Plate 1b are not sensitive to changes in dissolution flow rates.

### 4.3. Relative Permeability Relationship

As for the other functional relationships, relative permeabilities [see *Rajaram et al*., 1997; *Fischer and Celia*, 1999] can also be extended to cover the range of residual phase dissolution. Computed relative permeability results are presented in Plate 1c. The nonwetting phase has zero relative permeability at and below residual saturation, since it exists only as disconnected ganglia trapped by capillary forces. We do not consider ganglion mobilization by high capillary number flows in this investigation. The wetting phase relative permeability displays a monotonically increasing extension, with a change in slope at the point of residual saturation. An initial increase in wetting-phase saturation is seen prior to a significant response in relative phase permeability. We relate this observation to the trapping of interfaces in pore throats. The nonwetting-phase volumes in these throats are dissolved at first without altering the pathways or permeability to flow in the network, because a throat becomes available to flow only when it is occupied completely by wetting fluid. For the simulation, permeabilities are recomputed at times of full dissolution of the nonwetting phase from pore spaces.

The plotted relative permeability curves in Plate 1c fall closely together for the three flow rates. A consistent trend of higher permeabilities at the same saturation value is seen for the lower flow rates, underlining the differences in dissolution sequence apparent in Plate 1a. However, it has a minor effect here.

## 5. Conclusion

We have used a pore-scale network model that includes quasi-static capillary displacement, interphase mass transfer across fluid-fluid interfaces, and subsequent dynamic retraction of interfaces due to the mass transfer to extend the constitutive relationships for two-phase flow. We computed extensions for the relationships between capillary pressure and saturation, between relative permeability and saturation, and between specific fluid-fluid interfacial area and saturation for a single set of pore structure parameters and three fluid velocities. To do this, we employed a modified definition of capillary pressure, involving areal averaging of local pressure differences along all fluid-fluid interfaces. This allows the capillary pressure definition to apply to all ranges of saturations, because it involves the actual pressures internal to a sample, as opposed to the external reservoir pressures. In the extended range the $p^c - s^w$ relationship does not remain monotonic. Therefore incorporation of this relationship in standard two-phase models that employ derivatives of $p^c - s^w$ should be avoided. In general, we believe that more careful consideration should be given to the definition of capillary pressure in standard continuum-scale model formulations, while further research is needed to determine the general suitability of the current equations employed to model two-phase flow systems.

The relationships between $a^{wn}$ and $s^w$, and between $k_r$ and $s^w$, are better behaved than the $p^c - s^w$ relationship, showing smooth curves and little dependence on the flow rate used during the dissolution process. The extent to which flow rates and other system dynamics need to be included in constitutive considerations is an open question and needs further investigation. Our results are presented for a particular choice of a pore-scale network model with a particular pore space structure. While many more simulations need to be run, we expect the qualitative behavior to remain similar over a wide range of pore structures. This would be consistent with the general behavior observed for the traditional $p^c - s^w$ and $k_r - s^w$ relationships, which remain qualitatively comparable for a wide range of materials.

In current macroscale models, $k_r$ and $a^{wn}$ are needed to solve problems involving dissolution, but the use of $p^c - s^w$ may be avoided in the saturation range of residual dissolution. However, newer theories like those of *Gray and Hassanizadeh* [1991, 1998] may require a well-defined $p^c$ over all $s^w$, and therefore extensions of $p^c - s^w$, as well as $k_r - s^w$ and $a^{wn} - s^w$, and perhaps others, will be needed. Computational pore-scale models provide a means to investigate these relationships.

**Acknowledgments.** This work was supported in part by the National Science Foundation under grants EAR-9218803 and EAR-9805376 and the Department of Energy under grant DE-FG07-96ER14703, and TU Delft, The Netherlands, provided support to M. Celia. Paul Reeves provided the capillary displacement code. The authors acknowledge the insightful comments and suggestions of S. Majid Hassanizadeh. We thank Helge Dahle, Lin Ferrand, William Gray, Carlo Montemagno, and Paul Reeves for helpful discussions and comments regarding this work.

## References

Dullien, F. A. L., F. S. Y. Lai, and I. F. MacDonald, Hydraulic continuity of residual wetting phase in porous-media, *J. Colloid Interface Sci*., *109*(1), 201–218, 1986.

Ewing, R. P., and S. C. Gupta, Pore-scale network modeling of compaction and filtration during surface sealing, *Soil Sci. Soc. Am. J*., *58*, 712–720, 1994.

Fischer, U., and M. A. Celia, Prediction of relative and absolute permeabilities for gas and water from soil water retention curves using a pore-scale network model, *Water Resour. Res*., *35*(4), 1089–1100, 1999.

Gray, W. G., and S. M. Hassanizadeh, Unsaturated flow theory including interfacial phenomena, *Water Resour. Res*., *27*(8), 1855–1863, 1991.

Gray, W. G., and S. M. Hassanizadeh, Macroscale continuum mechanics for multiphase porous-media flow including phases, interfaces, common lines and common points, *Adv. Water Resour*., *21*(4), 261–281, 1998.

Gvirtzman, H., and P. V. Roberts, Pore-scale spatial analysis of two immiscible fluids in porous media, *Water Resour. Res*., *27*(6), 1165–1176, 1991.

Harris, C. C., and N. R. Morrow, Pendular moisture in packings of equal spheres, *Nature*, *203*, 706–708, 1964.

Hassanizadeh, S. M., and W. G. Gray, Mechanics and thermodynamics of multiphase flow in porous media including interphase boundaries, *Adv. Water Resour*., *13*(4), 169–186, 1990.

Hassanizadeh, S. M., and W. G. Gray, Toward an improved description of the physics of 2-phase flow, *Adv. Water Resour*., *16*(1), 53–67, 1993a.

Hassanizadeh, S. M., and W. G. Gray, Thermodynamic basis of capillary pressure in porous media, *Water Resour. Res*., *29*(10), 3389–3405, 1993b.

Held, R. J., and M. A. Celia, Pore-scale modeling and upscaling of nonaqueous phase liquid mass transfer, *Water Resour. Res*., in press, 2000.

Li, Y., and N. C. Wardlaw, The influence of wettability and critical pore-throat size ratio on snap-off, *J. Colloid Interface Sci*., *109*(2), 461–472, 1986a.

Li, Y., and N. C. Wardlaw, Mechanisms of nonwetting phase trapping during imbibition at slow rates, *J. Colloid Interface Sci*., *109*(2), 473–486, 1986b.

Lowry, M. I., and C. T. Miller, Pore-scale modeling of nonwetting-phase residual in porous media, *Water Resour. Res*., *31*(3), 455–473, 1995.

Miller, C. T., G. Christakos, P. T. Imhoff, J. F. McBride, J. A. Pedit, and J. A. Trangenstein, Multiphase flow and transport modeling in heterogeneous media: Challenges and approaches, *Adv. Water Res*., *21*(2), 77–120, 1998.

Mohanty, K. K., H. T. Davis, and L. E. Scriven, Physics of oil entrapment in water-wet rocks, *SPE Reservoir Eng*., *2*(1), 113–127, 1987.

Morrow, N. R., Physics and thermodynamics of capillary action in porous media, *Ind. Eng. Chem. Res*., *62*(6), 32–56, 1970.

Morrow, N. R., and C. C. Harris, Capillary equilibrium in porous media, *SPE J*., *5*, 15–24, 1965.

Rajaram, H., L. A. Ferrand, and M. A. Celia, Prediction of relative permeabilities for unconsolidated soils using pore-scale network models, *Water Resour. Res*., *33*(1), 43–52, 1997.

Reeves, P. C., The development of pore-scale network models for the simulation of capillary pressure-saturation-interfacial area-relative permeability relationships in multi-fluid porous media, Ph.D. dissertation, 566 pp., Princeton Univ., Princeton, N. J., 1997.

Reeves, P. C., and M. A. Celia, A functional relationship between capillary pressure, saturation, and interfacial area as revealed by a pore-scale model, *Water Resour. Res*., *32*(8), 2345–2358, 1996.

Saripalli, K. P., P. S. C. Rao, and M. D. Annable, Determination of specific NAPL-water interfacial areas of residual NAPLs in porous media using the interfacial tracers technique, *J. Contam. Hydrol*., *30*, 375–391, 1998.

M. A. Celia and R. J. Held, Environmental Engineering and Water Resources Program, Department of Civil and Environmental Engineering, Princeton University, Princeton, NJ 08544. (celia@princeton.edu; held@karst.princeton.edu)

(Received July 26, 1999; revised July 31, 2000;
accepted July 31, 2000.)